Identification and quantitative evaluation of compensating Zn-vacancy–donor complexes in ZnSe by positron annihilation

J. Gebauer* and R. Krause-Rehberg
Fachbereich Physik, Martin-Luther-Universität Halle-Wittenberg, D-06099 Halle, Germany

M. Prokesch
Institute for Materials Research, Tohoku University, Sendai 980-8577, Japan

K. Irmscher
Institut für Kristallzüchtung (IKZ), Max-Born-Strasse 2, D-12489 Berlin, Germany
(Received 30 April 2002; revised manuscript received 19 July 2002; published 26 September 2002)

We investigate defects in *n*-type ZnSe bulk crystals by positron annihilation. With positron lifetime spectroscopy, vacancies with a positron lifetime of (280 ± 1) and (275 ± 10) ps were found in ZnS:I and ZnSe:Al, respectively. The positron bulk lifetime was 241 ps at 300 K, determined in an undoped semi-insulating reference. The vacancies were identified to be Zn-vacancy–donor complexes by combining the positron lifetime measurements with that of the positron-electron annihilation momentum distribution. This finding is supported by previous electron-paramagnetic-resonance measurements. The samples exhibited different degrees of electrical compensation, adjustable by thermal treatment under defined Zn vapor pressure. The vacancy concentration measured by positron annihilation could explain the deactivation of donors quantitatively. Thus, compensation of *n*-type conductivity in ZnSe is due to self-compensation through native Zn-vacancy–donor complexes.

DOI: 10.1103/PhysRevB.66.115206 PACS number(s): 61.72.Ji, 78.70.Bj

I. INTRODUCTION

The wide-band-gap semiconductor ZnSe attracted large attention as a potential material for light-emitting devices in the blue-green spectral range.[1] However, ZnSe devices, usually heteroepitaxially grown on GaAs substrates, suffer from fast degradation processes. Homoepitaxy on ZnSe substrates could prevent one source for such degradation. This requires ZnSe bulk crystals with good quality and reproducible electrical properties.

ZnSe bulk crystals often suffer from severe electrical compensation. One explanation would be self-compensation through native defects.[1] However, some theoretical calculations suggested that the formation energy of native defects would be too high to make them a source of any significant compensation in ZnSe.[2,3] Contrarily, other calculations yielded low formation energies for vacancy-dopant complexes, i.e., V_{Se}-acceptor and V_{Zn}-donor pairs in *p*- and *n*-type ZnSe, respectively.[4,5]

Experimentally, considerably few data exist on the microscopic nature of compensating native defects in ZnSe although defects introduced by electron irradiation into ZnSe are among the most studied defects at all.[6–8] Native V_{Zn}-Cl and V_{Zn}-I complexes, the so-called A centers, were identified with electron paramagnetic resonance (EPR).[8–10] However, it was later pointed out that the concentration of these complexes might not be large enough to explain the compensation observed.[1]

Positron annihilation (PA) is a technique especially sensitive to vacancy defects,[11] making it an ideal tool to clarify the above questions. During diffusion in a solid, positrons can be localized by vacancies prior to annihilation with an electron. This results in an increase of the positron lifetime and a change of the annihilation momentum distribution, allowing the sensitive detection of vacancies.[11]

Recent PA research on ZnSe focused on the investigation of epitaxial layers. Vacancy defects were found in undoped,[12] gallium-[13] and chlorine-[14]doped *n*-type, and nitrogen-doped *p*-type layers.[14–16] They were assigned to V_{Zn} and V_{Se}, respectively. In these studies, only the annihilation momentum distribution could be observed. The momentum distribution depends on the size *and* on the concentration of a defect. This information cannot be independently extracted.[11] Therefore, it cannot be finally decided if the defects observed are really monovacancies, larger agglomerates, or if they form complexes with the dopants. This makes assignment and quantification unreliable.

A detailed identification of defects by PA can be obtained by combining measurements of the momentum distribution with positron lifetime spectroscopy.[17–19] In practice, positron lifetime measurements must usually be done on bulk samples. Such measurements could be used as a reference for studies of thin epitaxial layers. However, very few positron studies of defects in bulk ZnSe samples exist. Positron lifetimes of 230 (Ref. 20) or 240 ps (Refs. 16, 21, and 22) were related to defect-free ZnSe while defect-related positron lifetimes of 300–325 ps were attributed to either Zn monovacancies[22] or divacancies.[20]

A particular problem for previous PA studies appears to be the lack of suitable, well-characterized bulk sample material. In the present work, we investigate *n*-doped [with iodine (I) and aluminum (Al)] and undoped ZnSe bulk crystals, previously studied by electrical methods and EPR.[23,24] We combine positron lifetime spectroscopy with measurements of the annihilation momentum distribution. In a preliminary study, using positron lifetime spectroscopy only, we found a

TABLE I. Specifications and positron lifetimes of the ZnSe samples investigated in the present work. Insulating behavior corresponds to a resistivity $>10^9\ \Omega$ cm, the detection limit of our setup.

Sample	Dopant with concentration	Carrier concentration (cm^{-3})	τ_{av} at 300 K (ps)	τ_{def} at 300 K (ps)	Remarks
ZnSe:I, insulating	I $(7\pm3)\times10^{18}$ cm^{-3}	insulating	279 ± 1	same as τ_{av}	as grown
ZnSe:I, conductive	I $(7\pm3)\times10^{18}$ cm^{-3}	1×10^{18}	281 ± 1	same as τ_{av}	annealed at 1040 °C, $p_{Zn}=3.9$ atm
ZnSe:Al, conductive	Al	2.4×10^{17}	244 ± 1	280 ± 8	Al indiffusion at 1000 °C for 4 days in Zn/0.02% Al melt
ZnSe:Al, insulating	Al	insulating	249 ± 1	272 ± 12	annealing in vacuum at 700 °C for 2 h
Horizontal Bridgman (HB), conductive	Unknown, probably unintentional Al impurities	4.9×10^{16}	244 ± 1	274 ± 11	annealing in Zn melt at 1000 °C for 4 days
HB, insulating		insulating	241 ± 1		annealing in vacuum at 700 °C for 2 h
ZnSe reference		insulating	241 ± 1		as grown by solid-state recrystallization

high density of vacancies in ZnSe:I.[23] In the present work, we show that the vacancies in *n*-ZnSe can directly be identified to be V_{Zn} monovacancies forming complexes with the donors, in accordance with EPR. Our results are in line with the assumption of self-compensation through native defects.

II. ZnSe SAMPLE MATERIAL

All ZnSe samples investigated in this work were bulk crystals. Iodine-doped material was grown by seeded chemical vapor transport at 830 °C using I as the transport agent.[25] The growth results in the incorporation of I with a concentration of $(7\pm3)\times10^{18}$ cm^{-3} (determined by instrumental photon activation analysis). Al-doped ZnSe was obtained by Al indiffusion from a Zn/Al melt into nominally undoped Bridgman-grown crystals.

The ZnSe:I samples were semi-insulating after growth (resistivity $>10^9\ \Omega$ cm) although I is a donor in ZnSe. Annealing under Zn vapor increased the room-temperature electron concentration n_e (determined by Hall-effect measurements) up to $n_e=1.4\times10^{18}$ cm^{-3} ($p_{Zn}\sim5$ atm).[23] The change in conductivity was completely reversible, and annealing of the same samples under lower Zn vapor pressure reduced the carrier concentration again (e.g., 7×10^{15} cm^{-3} at $p_{Zn}=2\times10^{-4}$ atm). n_e was proportional to the square root of the Zn vapor pressure. ZnSe:Al was *n*-type after indiffusion of Al. However, n_e was also proportional to the square root of the Zn vapor pressure applied during later annealing. The high electron concentration after indiffusion of Al is related to the high Zn vapor pressure over the Zn/Al melt.

The reversibility of n_e and its direct dependence on the Zn vapor pressure strongly suggests that a native defect is the compensating species. A natural candidate is the twofold negatively charged Zn vacancy. The Zn vacancy thermal equilibrium concentration is determined by the reaction $Zn(g)+V_{Zn}^{2-}\leftrightarrow Zn_{Zn}+2e^-$. The corresponding mass action law yields the experimentally observed square-root dependence of n_e on p_{Zn} in the region of high compensation.[23]

Under illumination with light of an energy above 2 eV typical EPR spectra were observed in ZnSe:I and ZnSe:Al.[23,24] The analysis showed that the spectra arise from Zn-vacancy–donor complexes (A centers) as identified earlier.[8,9] This finding is compatible with the above results with the simple assumption that the complexes form only during cooling but are dissociated at high temperatures. Unfortunately, only a fraction of the A centers could be recharged by illumination to the neutral, paramagnetic state visible with EPR. Therefore, no quantitative information could be obtained, i.e., it was not clear if the A centers can explain the electrical compensation.[24]

In the present study, we investigate three sets of *n*-type ZnSe samples (see also Table I): (i) ZnSe:I with an I concentration of $(7\pm3)\times10^{18}$ cm^{-3}, as-grown (insulating) and annealed at 1040 °C, $p_{Zn}=3.9$ atm ($n_e=1\times10^{18}$ cm^{-3}). (ii) ZnSe:Al, obtained by diffusing Al into undoped Bridgman-grown crystals from a Zn/0.02%Al melt at 1000 °C for 4 days. The Zn vapor pressure over the melt is 2.8 atm. These samples were investigated in the as-diffused state ($n_e=2.4\times10^{17}$ cm^{-3}) and after annealing in vacuum at 700 °C for 2 h (insulating). (iii) Undoped Bridgman-grown ZnSe, annealed in a pure Zn melt at 1000 °C for 4 days ($n_e=4.9\times10^{16}$ cm^{-3}; the conductivity is most probably caused by unintentionally introduced impurities) and annealed in vacuum at 700 °C for 2 h (insulating). As a reference we investigated high-purity semi-insulating ZnSe grown by solid-state recrystallization, commercially obtained from Sumitomo Electric Industries, Ltd. For the purpose of defect identification with PA, we investigated polycrystalline pure (5*N*) Zn and Se reference samples.

III. POSITRON ANNIHILATION

Prior to annihilation with an electron in a solid, positrons may be trapped in vacancies. This results in an increase of the positron lifetime and a narrowing of the electron-positron annihilation momentum distribution compared to annihilation in defect-free material. These effects can be used to determine type and concentration of vacancies.[11]

Positron lifetime spectroscopy was performed using a

conventional system (time resolution: 250 ps full width at half maximum). A ^{22}NaCl positron source (activity: 40 μCi, covered by 1.5-μg/cm^2 Al foil) was placed between a pair of identical samples. We collected $3-6\times10^6$ events in each lifetime spectrum. The temperature T was varied between 30 and 600 K. For the measurements, T was cycled as 300 $\rightarrow$30$\rightarrow$600$\rightarrow$300 K in order to exclude unwanted temperature effects such as defect annealing influencing the results.

After source and background corrections, the positron lifetime spectra $n(t)$ were fitted according to the positron trapping model with a sum of exponential decay components

$$n(t)=n_0\sum_i I_i/\tau_i \exp(-t/\tau_i) \tag{1}$$

convoluted with the Gaussian resolution function of the spectrometer. n_0 is the total number of observed annihilation events and I_i is the relative intensity of the component with the positron lifetime τ_i. From the decomposition, the average positron lifetime $\tau_{\rm av}$ was obtained as the superposition

$$\tau_{\rm av}=\sum_i I_i\tau_i, \tag{2}$$

which is not sensitive to the numerical uncertainties of the spectra decomposition.

In a defect-free sample, positrons annihilate with a characteristic single lifetime $\tau_{\rm bulk}$. If positrons are trapped in vacancy defects, an additional characteristic lifetime for each defect type is present in the spectrum. The defect-related positron lifetime in vacancies is larger than $\tau_{\rm bulk}$. Thus, $\tau_{\rm av}$ increases above $\tau_{\rm bulk}$ if positrons are trapped at vacancies. From the spectra decomposition, one can calculate the theoretical bulk lifetime $\tau_b^{\rm TM}$

$$1/\tau_b^{\rm TM}=\sum_i I_i/\tau_i. \tag{3}$$

If the model assumptions (most important: the number of positron lifetime components) are correct, $\tau_b^{\rm TM}$ agrees with the independently determined positron bulk lifetime $\tau_{\rm bulk}$.

If only one type of vacancy traps positrons, the positron lifetime spectra have two components. The longer positron lifetime $\tau_{\rm def}$ is the characteristic positron lifetime due to annihilation in the vacancies. The first component τ_1 is given by $(1/\tau_1=1/\tau_{\rm bulk}+\kappa_{\rm vac})$, where $\kappa_{\rm vac}$ is the trapping rate into vacancies. $\kappa_{\rm vac}$ can also be obtained from

$$\kappa_{\rm vac}=\frac{1}{\tau_{\rm bulk}}\frac{(\tau_{\rm av}-\tau_{\rm bulk})}{(\tau_{\rm def}-\tau_{\rm av})}=\mu_{\rm vac}c_{\rm vac}. \tag{4}$$

The trapping rate is directly related to the vacancy concentration $c_{\rm vac}$ by the trapping coefficient $\mu_{\rm vac}$, which is specific for a given defect. The trapping coefficient is 10^{15} s^{-1} with an uncertainty of $\sim$50% for negatively charged monovacancies in semiconductors at 300 K.[26]

The positron lifetime depends mainly on the electron density and thus gives information on the open volume of a defect. At high momentum p_L, the electron-positron annihilation momentum distribution is dominated by annihilation with core electrons. Shape and intensity of the momentum distribution can therefore be used to study the chemical surrounding of defects.[17,18] The annihilation momentum distribution $f(p_L)$ is the superposition of annihilation from the different annihilation states, i.e.,

$$f(p_L)=n_{\rm bulk}f_{\rm bulk}(p_L)+\sum_j \eta_j f_j(p_L), \tag{5}$$

where the η are the normalized fractions of positrons annihilating in the bulk and in defect j. The η can be obtained from the decomposition of positron lifetime spectra measured under the same conditions. For the case of one defect type, the fraction of positrons annihilating in vacancies $\eta_{\rm vac}$ is given by $\eta_{\rm vac}=\kappa_{\rm vac}/(\tau_{\rm bulk}^{-1}+\kappa_{\rm vac})$. $\tau_{\rm av}$ can be expressed equivalent to $f(p_L)$, i.e., $\tau_{\rm av}$ is $(\eta_{\rm bulk}\ \tau_{\rm bulk}+\Sigma\,\eta_j\tau_j)$.

We observed the momentum distribution by coincidence spectroscopy using a setup of two Ge detectors.[27] In each spectrum, 1.5×10^7 coincident events were collected. All measurements of the momentum distribution were performed at room temperature (300 K). The intensity of the annihilation with core electrons was characterized by the W parameter defined as the relative intensity in the momentum range $p_L=(15-20)\times10^{-3}$ m$_0$c. W will be normalized to the value $W=0.008\,73$ of a ZnSe reference free from positron trapping into vacancies. For comparison, we determined the often used S parameter, defined as the relative intensity in the momentum range $p_L=(0-3)\times10^{-3}$ m$_0$c. S is normalized to the reference value 0.504.

IV. RESULTS

A. Positron lifetime spectroscopy

Figure 1 shows the positron lifetime as a function of temperature for ZnSe:I in comparison to a semi-insulating ZnSe reference. In the reference, the average positron lifetime ($\tau_{\rm av}$) increases slightly with increasing temperature. The positron lifetime spectra were single component. At 300 K, a positron lifetime of (241 ± 1) ps is found. We attribute this value to the positron lifetime $\tau_{\rm bulk}$ in ZnSe free from positron trapping at vacancies, in agreement with earlier results.[16,21,22] $\tau_{\rm av}$ increases slightly by $\sim$2.4 ps from 100 to 550 K. A similar behavior of the positron lifetime is observed in other semiconductors, e.g., GaAs, where it is attributed to thermal lattice expansion. In GaAs, $\tau_{\rm bulk}$ increases by $\sim$1.5 ps from 100 to 550 K.[28] In ZnSe, that increase can be expected to be larger due to the larger thermal expansion coefficient of ZnSe,[29] compared to GaAs.

In the I-doped samples, the average positron lifetime is well above that in the reference. This shows clearly the presence of vacancy defects. $\tau_{\rm av}$ increases with temperature from $\sim$270 (at 20 K) to $\sim$283 ps (at 550 K). Only minor differences are found between the as-grown, insulating, and annealed, conductive samples. At 300 K, $\tau_{\rm av}$ is (280 ± 1) ps. The spectra could not be decomposed into lifetime components, i.e., only one positron lifetime (corresponding to $\tau_{\rm av}$) is present. The variance of the positron lifetime fit is scattered randomly from 1.0 to 1.15 in the whole temperature range, i.e., close to the ideal value. If a second lifetime com-

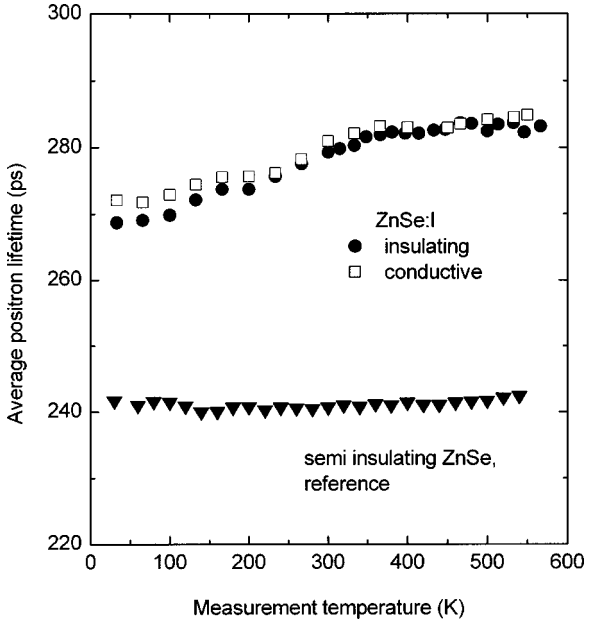

FIG. 1. Average positron lifetime as a function of the measurement temperature for insulating (as-grown) and conductive (annealed at $p_{Zn}=3.9$ atm) ZnSe:I in comparison to an undoped, semi-insulating ZnSe reference.

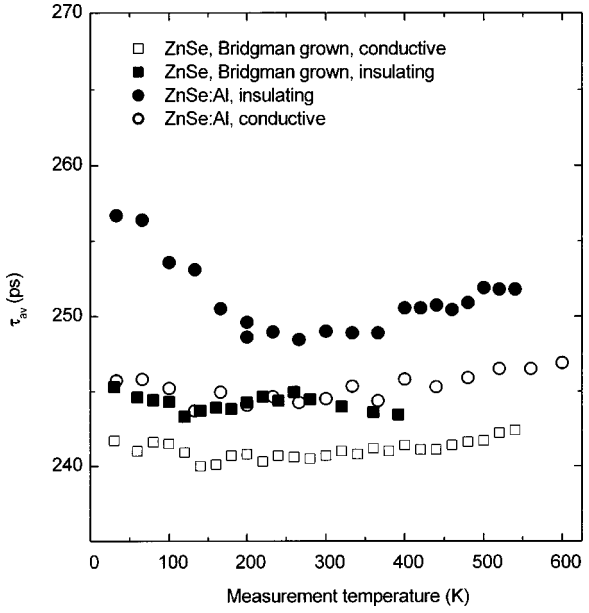

FIG. 2. Average positron lifetime as a function of the measurement temperature for ZnSe:Al and nominally undoped, Bridgman-grown ZnSe, insulating (annealed in vacuum) or conducting (annealed in a Zn melt).

ponent would be present, a significantly higher variance (about two or larger) is expected (see, e.g., Ref. 11, and references therein). Note that another type of vacancy with a similar defect-related positron lifetime would probably not be detectable in the lifetime fit. However, the measurements of the momentum distribution below and especially considerations of the defect chemistry and the electrical measurements[23,24] require that only one defect type be present.

The decrease of τ_{av} to low temperatures is often observed when positron trapping at vacancies compete with that in negative ions.[30] The ions can bind positrons in their shallow Coulomb potential only at low temperatures with annihilation parameters close to the bulk values. With decreasing temperature, more positrons annihilate at the ions, thus leading to a decrease of τ_{av}. This lifetime is usually too close to the vacancy lifetime to be resolvable, i.e., the lifetime fit yields only one positron lifetime. At very low temperatures (25 K), positrons cannot escape trapping at the ions and a steady state of competing trapping at ions and vacancies is reached. Then, the concentration of negative ions can be estimated from a simple two-defect trapping model with the equation

$$\kappa_{ion}(25\ \mathrm{K}) = c_{vac}\mu_{vac}(25\ \mathrm{K})\frac{[\tau_{vac}-\tau_{av}(25\ \mathrm{K})]}{[\tau_{av}(25\ \mathrm{K})-\tau_{bulk}]} - \tau_{bulk}^{-1} = \mu_{ion}(25\ \mathrm{K})c_{ion}, \quad (6)$$

where κ_{ion}, μ_{ion}, and c_{ion} are the trapping rate, trapping coefficient, and concentration of the negative ions, respectively. The vacancy concentration is estimated to be $>3\times10^{18}$ cm^{-3} using Eq. (1) from the data at high temperatures (>500 K) where trapping into negative ions is negligible[30] (see below). With $\tau_{vac}=280$ ps, $\tau_{bulk}=240$ ps, and $\mu_{ion}(25\ \mathrm{K})=\mu_{vac}(25\ \mathrm{K})=10^{16}$ s^{-1} (Ref. 26) we obtain an ion concentration of 1.2×10^{18} cm^{-3}, i.e., in the same order as the vacancy concentration.

We will show below that the vacancy concentration is high enough to explain all the electric compensation observed in ZnSe:I, excluding similar high concentrations of negative ions present. The concentration of negative ions must be significantly lower than the vacancy concentration in order to be consistent with the electrical measurements.[23,24] The discrepancy can be resolved by considering that the trapping coefficient for negative ions in ZnSe is not exactly known, making quantitative estimations uncertain within at least an order of magnitude.[11,26] We have to conclude that either the trapping coefficient of the ions must be much higher than previously believed (i.e., $\mu_{ion}(25\ \mathrm{K})\gg10^{16}$ s^{-1}) or the positron lifetime data must be explained without invoking negative ions. It is interesting to note that Dannefaer and Pu[31] recently calculated a similar temperature dependence of τ_{av} as we observed in ZnSe:I but without invoking negative ions in contrast to previous assumptions.[11,30] A decrease of τ_{av} toward low temperatures is predicted for high vacancy concentrations which would be in agreement with our results.

In Fig. 2, τ_{av} is shown for the Al-doped and -undoped samples. In the undoped, conductive sample, τ_{av} closely matches the positron lifetime in the reference, indicating that the vacancy concentration is below the detection limit of PA [$\sim3\times10^{15}$ cm^{-3}, estimated using Eq. (4) with a trapping coefficient of 10^{15} s^{-1}]. In the other samples, τ_{av} is higher than the reference value, showing the presence of vacancy defects. In these samples, τ_{av} decreases slightly with temperature from 550 to 200 K. This behavior is very similar to that one in the reference sample. We attribute it therefore to

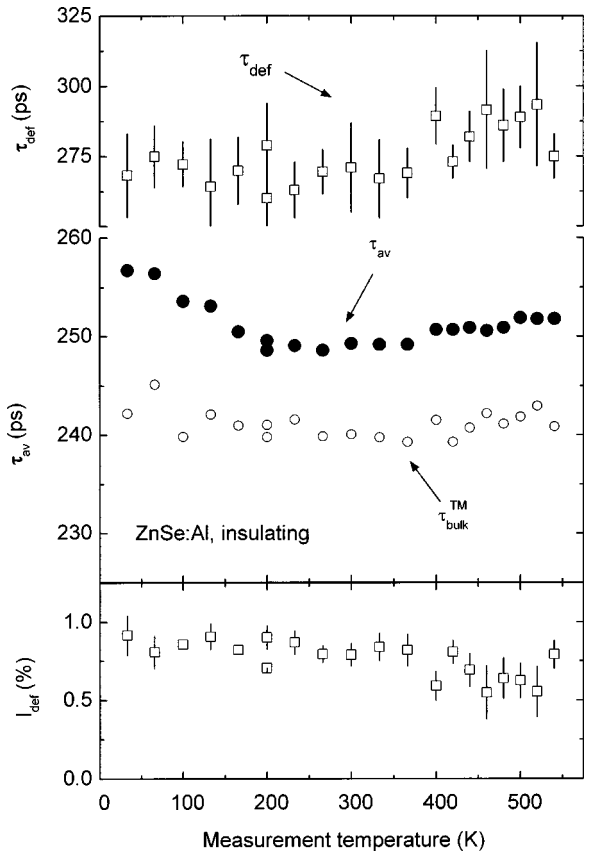

FIG. 3. Two-component decomposition of the positron lifetime spectra in the insulating ZnSe:Al sample. τ_{def} is the second lifetime component, associated with positron annihilation in the vacancies. The intensity I_{def} of that lifetime component is shown in the lower part. τ_b^{TM} is the lifetime in defect-free ZnSe, calculated from the decomposition according to a two-state trapping model. τ_b^{TM} is in good agreement with the measured bulk lifetime shown in Fig. 1.

thermal lattice expansion, too, as mentioned above. However, τ_{av} increases when the temperature is further decreased. The increase observed at low temperatures is most pronounced in the Al-doped, insulating sample. According to theory, positron trapping in negative vacancies increases with decreasing temperature but is constant for neutral vacancies.[32] Therefore, at least a part of the detected vacancies must be negatively charged.

The positron lifetime spectra could be decomposed into two components. In Fig. 3, the decomposition is exemplarily shown for the Al-doped, insulating sample. The longer lifetime component, τ_{def}, was (272 ± 12) ps at 300 K and increases slightly with temperature. This lifetime is related to positron annihilation at the vacancies. The intensity of τ_{def} was $\sim$60% at high temperatures and increases to $\sim$80% toward low temperatures. From the decomposition, we calculated the positron lifetime τ_b^{TM} using Eq. (3) (open circles in Fig. 3). τ_b^{TM} coincides with the experimental bulk lifetime determined in the reference (Fig. 1), indicating that the positron lifetime spectra can be sufficiently described with a trapping model considering one type of vacancy defect.[11]

The same defect-related positron lifetime as in insulating ZnSe:Al was found in the other Al-doped sample and in the undoped insulating sample within the margin of error. The average value of τ_{def} was (275 ± 10) ps at 300 K. This defect-related lifetime is close to the average positron lifetime in ZnSe:I (Fig. 1), indicating the same defect type. It is interesting to note that even the temperature dependence of τ_{def} in Fig. 3 is similar to that of τ_{av} in Fig. 1. This offers an alternative explanation for the temperature dependence of τ_{av} in ZnSe:I, avoiding the necessity to invoke negative ions. We found a similar temperature dependence of the defect-related lifetime for donor–Ga-vacancy complexes in GaAs.[19] This behavior might be related to thermal lattice expansion, too, although the increase of τ_{def} is larger that expected from that effect alone. Nevertheless, the statistical errors of the positron lifetime fit does not allow definite conclusions on that point.

The ratio between τ_{def} and τ_b is $\sim$1.16. This is a typical value for monovacancies in semiconductors.[11] In addition, the vacancy concentration changes with p_{Zn}. Simple defect chemical considerations show that, in equilibrium, this can only be true for monovacancies but not for the next largest defect type, divacancies. Therefore, the defects detected by positron annihilation are monovacancies.

The average positron lifetime, i.e., also the vacancy concentration, is lower in the respective conductive samples prepared under high Zn vapor pressure. This is a strong indication for Zn vacancies. The concentration of Se vacancies would increase with increasing p_{Zn}. At first glance, the I-doped samples seem not to fit into this trend because τ_{av} is not changed after annealing. We will show below that this is due to saturated positron trapping. It does not indicate that the vacancy concentration is constant.

To summarize the findings of positron lifetime spectroscopy, we find a bulk lifetime of (241 ± 1) ps in ZnSe. In *n*-doped ZnSe, we find negatively charged vacancies with a positron lifetime at 300 K of (280 ± 1) ps (in ZnSe:I) and (275 ± 10) ps (in ZnSe:Al and undoped HB-grown ZnSe). The defects are attributed to Zn monovacancies due to their reduced abundance under Zn-rich conditions.

B. Annihilation momentum distribution

As the next step, we performed measurements of the annihilation momentum distribution at 300 K. First, we confirm that indeed the same defect type is present in all samples. For that purpose, the correlation between the *W* parameter and average positron lifetime was observed. The fraction of positrons annihilating in vacancies η_{vac} is given by

$$\eta_{\mathrm{vac}}=(W_b-W)/(W_b-W_{\mathrm{def}})=(\tau_{\mathrm{av}}-\tau_b)/(\tau_{\mathrm{def}}-\tau_b) \quad (7)$$

for the case of one defect type. The measured *W* parameter depends thus linearly on τ_{av} if the defect density changes (which is directly related to η_{vac}) and not the defect type (i.e., τ_{def} or W_{def}).[33] In Fig. 4, the measured normalized *W* parameter is plotted vs τ_{av}. Within the errors, all data follow the same linear variation (indicated by the solid line). The agreement shows that the vacancies all belong to the same type. W_{def} was determined to be $W_{\mathrm{def}}=(0.73\pm0.01)$. However, the W-τ_{av} analysis does not allow to distinguish between isolated vacancies and vacancies in a complex with

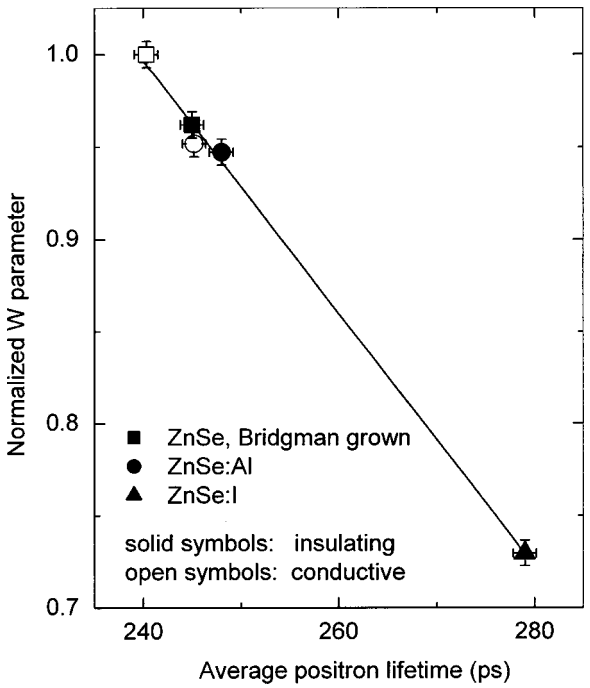

FIG. 4. Normalized *W* parameter as a function of the average positron lifetime, both measured at 300 K, for the ZnSe samples investigated in this work.

foreign atoms.[19,33] For comparison, also the *S* parameter was measured. *S* behaved as τ_{av} (not shown). The *S* parameter for annihilation in the vacancies was $S_{def}=(1.022\pm0.01)$, a typical value for monovacancies in semiconductors.[11]

The annihilation momentum distribution was then observed in detail to identify the chemical surrounding of the vacancies. For that purpose, we first establish suitable references. In Fig. 5(a), the momentum distribution is shown for pure Zn and Se in comparison to that of bulk ZnSe. In Fig. 5(b), the same data are shown but normalized by taking the ratio to bulk ZnSe. In the following discussion, only the annihilation with core electrons at $p_L>15\times10^{-3}m_0c$ is relevant.[17] For Zn, the intensity of the momentum distribution in that region is higher than in bulk ZnSe (ratio >1) while the momentum distribution is narrower than in bulk ZnSe, i.e., the ratio decreases toward high momentum. Contrarily, for Se the momentum distribution is less intense and broader than in bulk ZnSe, i.e., the ratio increases toward high momentum. The momentum distribution in bulk ZnSe is an average between that of Zn and Se as one would expect. The shape of the core annihilation momentum distribution is not significantly affected by the binding of an atom in a solid.[17,34] Therefore, the results for Zn and Se can be used as a reference to identify the chemical surrounding of defects in ZnSe.

The momentum distribution for the vacancies in ZnSe:I and ZnSe:Al is shown in Fig. 6. Only the normalized momentum distribution is shown and the momentum distribution for the vacancy in ZnSe:Al was shifted by -0.25 for clarity. Due to saturated positron trapping in ZnSe:I (Fig. 1), the momentum distribution characteristic for the vacancy corresponds directly to the measured one. The momentum

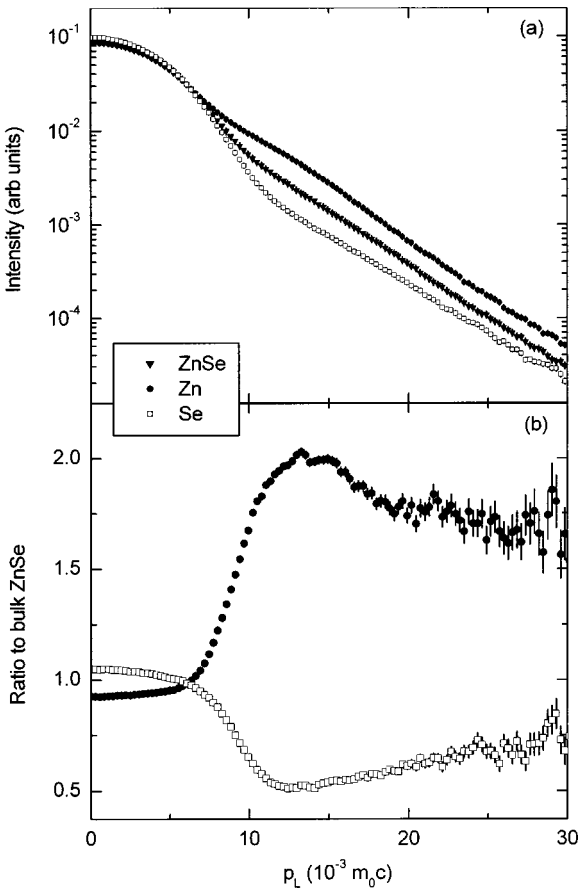

FIG. 5. (a) Annihilation momentum distribution in bulk ZnSe, pure Zn, and pure Se, measured at 300 K. (b) Annihilation momentum distribution in Zn and Se normalized by taking the ratio to that of bulk ZnSe.

distribution for the vacancy in ZnSe:Al was determined through measurements on the conductive ZnSe:Al sample. Here, ~25% of the positrons are trapped at the vacancies at 300 K. The characteristic momentum distribution for the vacancy was obtained from decomposing the measured one employing Eq. (5) with the known momentum distribution from bulk ZnSe (Fig. 5).

The momentum distribution of the vacancies (at $p_L>15\times10^{-3}m_0c$) has a lower intensity than in bulk ZnSe because the probability of annihilation with core electrons is reduced in vacancies. More importantly, the shape differs from that in the bulk ZnSe. The ratio increases toward high momentum, i.e., the annihilation momentum distribution of the vacancies is broader than that of bulk ZnSe. The shape is similar to that of Se but is clearly different from that of Zn [Fig. 5(a)]. Thus, annihilation in the vacancies occurs preferentially with electrons from Se, showing that the vacancies are surrounded predominately by Se atoms. Therefore, the vacancies in ZnSe:Al and ZnSe:I both belong to the Zn sublattice, consistent with the interpretation of the positron lifetime results.

A closer look shows that the core annihilation momentum distribution in ZnSe:Al is slightly different from that in ZnSe:I. In ZnSe:Al, it is very similar to that of Se, indicating a vacancy surrounded only by Se atoms. Because positron annihilation occurs predominantly with electrons from the

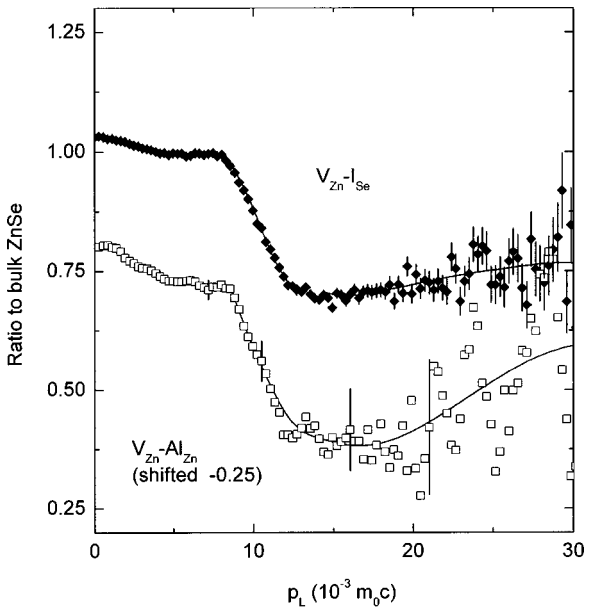

FIG. 6. Normalized annihilation momentum distribution for the vacancy in ZnSe:I and for the vacancy in ZnSe:Al. The vacancies are identified to be V_{Zn}-I_{Se} or V_{Zn}-Al_{Zn} complexes, respectively (see text). Solid lines are from data smoothing and serve to guide the eye only.

nearest-neighbor atoms, we cannot decide whether the vacancy in ZnSe:Al forms a complex with a second next neighbor on the Zn sublattice, i.e., with Al_{Zn}. However, isolated Zn vacancies should not be stable at room temperature according to previous investigations of irradiated ZnSe.[7,35] Moreover, V_{Zn}-Al_{Zn} complexes were previously found by EPR,[23,24] making V_{Zn}-Al_{Zn} the most probable assignment for the vacancies in ZnSe:Al. From a decomposition of the measured momentum distribution using Eq. (5), we obtained the same momentum distribution also for the Zn vacancies in the undoped, insulating Bridgman-grown ZnSe sample, confirming that the defect type is the same.

In ZnSe:I, the normalized momentum distribution increases less steeply toward high momentum than in ZnSe:Al, indicating a somewhat different chemical environment. This behavior must be explained by the presence of an atom different from Se next to the Zn vacancy. Because positrons ''see'' only the atoms closest to the vacancy, the foreign atom must reside on the Se sublattice. The most numerous foreign atoms in ZnSe:I are the I_{Se} donors. We attribute therefore the vacancies in ZnSe:I to V_{Zn}-I_{Se} complexes.

This assignment is corroborated by a consideration of the electrons contributing to the annihilation at high momentum. In Zn and Se, these are mainly $3d$ electrons.[18] The Se $3d$ electrons are more tightly bound than the Zn $3d$ electrons due to the higher atomic number of Se ($Z=34$ compared to 30 of Zn). The Se $3d$ electrons are therefore less localized in momentum space, i.e., the momentum distribution is broader and decays less steeply than that of Zn (Ref. 18) (Fig. 5). In I ($Z=53$), the main contribution to the core annihilation comes from $4d$ electrons. They are less strongly bound than the Se $3d$ electrons.[18] The resulting momentum distribution is therefore more localized in momentum space, i.e., it decays more steeply with an increased contribution at lower momentum (close to $15\times10^{-3}m_0c$). Such behavior is observed in Fig. 6 for ZnSe:I in contrast to the vacancy in ZnSe:Al, indicating V_{Zn}-I_{Se} complexes in ZnSe:I. In addition, the previous EPR experiments already demonstrated the presence of V_{Zn}-I_{Se} complexes in our samples,[23,24] in agreement with the assignment by positrons.

The results in ZnSe are analogous to our previous investigations of V_{Ga}-Te_{As} complexes in GaAs.[19] In that case, Te with core annihilation from $4d$ electrons replaces an As atom with core annihilation from $3d$ electrons adjacent to a Ga vacancy. This leads to a similar change of the momentum distribution while the difference is barely visible in the W-τ_{av} plot.[19]

To summarize this part, the observation of the momentum distribution confirms that the vacancies in ZnSe:I and ZnSe:Al both belong to the Zn sublattice. The Zn vacancies in ZnSe:I are found to form complexes with I donors. This result agrees with the previous identification of A centers by EPR.[23,24] From the PA measurements alone, we cannot decide whether the Zn vacancies in ZnSe:Al form complexes with the Al donors, too. However, in view of the previous EPR results,[23,24] the most probable assignment is V_{Zn}-Al_{Zn} complexes.

C. Vacancy-impurity complexes as compensating species

This section focuses on the question of whether the electrical compensation of donors can be explained by the V_{Zn} complexes. V_{Zn} is twofold negatively charged in n-ZnSe,[2,4] i.e., each complex compensates two singly charged donors. The vacancy concentration can be independently obtained from the measured trapping rate [Eq. (4)] provided the trapping coefficient μ_{vac} is known.

First, we consider ZnSe:I. Due to saturated positron trapping, only a lower limit of the positron trapping rate of $\sim6\times10^{10}$ s^{-1} can be estimated. The V_{Zn}-I_{Se} concentration is thus at least 2.6×10^{18} cm^{-3} according to Eq. (1) with a trapping coefficient of 10^{15} s^{-1} at 300 K.[26] The as-grown ZnSe:I sample is fully compensated. Thus, a vacancy concentration of 3.5×10^{18} cm^{-3} is expected (i.e., half of the donor concentration) if the V_{Zn}-I_{Se} complexes are the dominating compensating species. The measured vacancy concentration is in agreement with this assumption, i.e., the vacancies can explain the compensation quantitatively.

We are now also able to explain why the PA results are the same for insulating and conducting ZnSe:I. The carrier concentration is 1×10^{18} cm^{-3} in the conducting ZnSe:I sample, i.e., this sample is still strongly compensated. Therefore, there are still $\sim3\times10^{18}$-cm^{-3} V_{Zn}-I_{Se} complexes present (instead of 3.5×10^{18} cm^{-3} in the insulating sample). From Eq. (4), it can be easily calculated that this corresponds to a change of τ_{av} smaller than 1 ps. Such a small difference cannot be resolved with our lifetime spectrometer, i.e., the same PA results are expected for compensated and conducting ZnSe:I.

Finally, we check whether the electrical compensation in the ZnSe:Al and Bridgman-grown samples can be explained with vacancies as well. For that purpose, we compare the

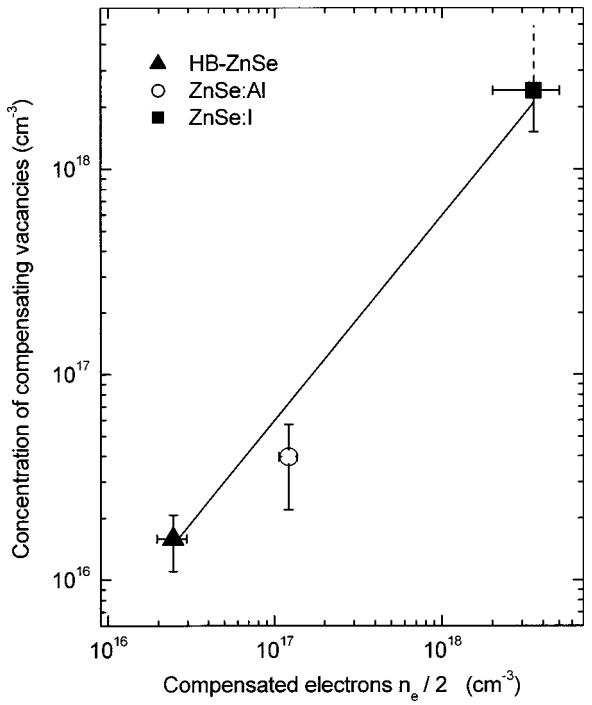

FIG. 7. Concentration of compensating vacancies as a function of the concentration of compensated electrons. The line is a linear fit to the data showing that the vacancies compensate the donors (see text).

vacancy concentration measured by PA with the concentration of compensated donors. Unfortunately, the absolute donor concentration n_{donor} is not known for the ZnSe:Al and Bridgman-grown samples. Therefore, we relate the difference of the carrier concentration between insulating and conducting samples (the concentration of compensated carriers Δn_e) to the corresponding difference of the vacancy concentrations (the concentration of compensating vacancies Δc_{vac}), i.e., $\Delta n_e/2 = \frac{1}{2} \times (n_e^{\mathrm{cond}} - n_e^{\mathrm{insul}})$ should equal $\Delta c_{\mathrm{vac}} = (c_{\mathrm{vac}}^{\mathrm{insul}} - c_{\mathrm{vac}}^{\mathrm{cond}})$. The factor $\frac{1}{2}$ takes into account that each complex compensates two donors. In ZnSe:I, the concentration of compensated carriers is simply equal to the known donor concentration and the concentration of compensating vacancies is given by the vacancy concentration in insulating, fully compensated material. In Fig. 7, the concentration of compensating vacancies is plotted versus half of the concentration of compensated electrons for all samples. The line in Fig. 7 is a linear fit to the data with $\Delta c_{\mathrm{vac}} = a \times \Delta n_e/2$ yielding $a = (0.7 \pm 0.1)$. The good agreement with the data shows that the vacancy complexes dominate the compensation. The factor a is the ratio between the actual trapping coefficient of the V_{Zn} complexes and that of 10^{15} s^{-1} used in Eq. (1). The discrepancy is well within the uncertainties of $\sim$50% for the trapping coefficient.[26] To summarize this part, we conclude that the V_{Zn} complexes observed by PA dominate the compensation of donors in *n*-ZnSe.

V. DISCUSSION

A. Carrier compensation

Our PA results show the existence of V_{Zn}-donor complexes in *n*-type ZnSe. Consistently with this finding, the existence of V_{Zn} complexes has been shown before by EPR.[24] The total vacancy concentration could not be determined by EPR,[23,24] but easily by PA. We found that the vacancy concentration can explain the electrical compensation of donor doping, i.e., we confirmed quantitatively that compensation in *n*-ZnSe is due to self-compensation through native Zn-vacancy–donor complexes (so-called A centers). This is in line with those theoretical calculations which predict that V_{Zn}-donor complexes have a low formation energy in *n*-doped ZnSe and should therefore be the dominating compensating species.[4]

The situation in ZnSe is analogous to that in GaAs. In both materials, acceptor-type cation vacancies have the lowest formation energy of all native defects at high *n*-doping under anion-rich conditions. The formation of these charged defects (self-compensation) becomes favorable if the formation energy of the neutral vacancy is lower than the energy gain due to electron transfer from the Fermi level to the accompanied acceptor level(s).[36] In ZnSe with its wider band gap, self-compensation can be complete, however, in GaAs always only a part of the donors is compensated.[37]

B. Positron annihilation parameter

The present work is the first combined positron lifetime/core annihilation momentum distribution study of defects in ZnSe. The defect identification is backed by EPR and electrical measurements. It is thus very interesting to compare our data to previous PA results. We found the following positron annihilation parameters for V_{Zn}-donor complexes: at 300 K (i) the positron lifetime is (280 ± 1) ps (for V_{Zn}-I_{Se}) or (275 ± 10) ps (for V_{Zn}-Al_{Zn}), (ii) the *W* parameter is (0.73 ± 0.01), and (iii) the *S* parameter is (1.022 ± 0.01). The positron lifetime in bulk ZnSe was found to be 241 ps.

Our bulk positron lifetime agrees with that found in Refs. 16, 21, and 22, giving credit to the assignment. Theoretical calculations gave bulk lifetimes of 233 ps using the local-density approximation (LDA),[38] or of 250.5 ps, using the generalized gradient approximation (GGA).[22] LDA calculations usually underestimate positron lifetimes while the GGA usually gives positron lifetimes within a few ps of the experimental values.[19,39] However, in the atomic superposition calculations employed in Ref. 22, the strong charge transfer between the atoms for II-VI compounds is not taken properly into account, resulting in too long positron lifetimes.[39] More accurate (shorter) positron lifetimes are expected when a self-consistent electron density is used within the GGA.[39] Our experimental positron bulk lifetime (241 ps) is just between that of the published calculations,[22,38] thus showing a good agreement.

Positron lifetimes of 245 (265) for V_{Zn}, 252 (279) for V_{Se}, and 310 (343) ps for $V_{Zn}V_{Se}$ divacancies were calculated using LDA (GGA), respectively.[22,38] Lattice relaxation was not considered. The calculated positron lifetimes for V_{Zn} are significantly shorter than our experimental ones for V_{Zn}-donor complexes. It is highly unlikely that the presence of the donors close to the vacancies increases the positron lifetime that much.[19] The remaining explanation for the discrepancy is thus an outward lattice relaxation. Such a relax-

ation is not found by EPR.[23,24] However, the trapped positron itself is known to influence the lattice relaxation by pushing the neighboring atoms outwards, thereby increasing the positron lifetime. This effect has been calculated in detail for V_{Ga} in GaAs, where it amounts to an outward relaxation of only a few percent.[40] In ZnSe with its ''soft'' lattice,[1] the effect can be expected to be considerably larger, thus providing an explanation for our results. Only a detailed *ab initio* calculation considering lattice relaxation can clarify this point. Nevertheless, the positron lifetime calculated for divacancies is far larger than our experimental results. Therefore, our data are only compatible with positron annihilation at monovacancies.

Only a few previous positron lifetime measurements of native defects in bulk ZnSe exist. A defect-related positron lifetime of (303 ± 13) ps was found by Tessaro and Mascher[20] and attributed to divacancies. Plazaola *et al.* found vacancies with a positron lifetime of (325 ± 5) ps, attributed to V_{Zn} or related complexes.[22] The defect-related lifetimes are significantly longer than our value of (275–280) ps. In both studies, however, no independent proof for the existence of V_{Zn} monovacancies (such as EPR) was available. Our results suggest that the defects in Refs. 20 and 22 are rather divacancies or larger vacancy complexes. It is interesting to note that these studies were done in undoped material. There, possibly existing Zn vacancies might not find enough partners (such as I donors) to form stable monovacancy complexes, leaving only larger agglomerates as stable vacancy-type defects.

Electron irradiation is a suitable way to introduce single point defects such as monovacancies. Pareja *et al.*[21] and Abgarjan *et al.*[35] found a defect-related positron lifetime of ~270 ps in ZnSe irradiated with electrons below room temperature. This lifetime was attributed to Zn monovacancies, in agreement with our finding and with earlier EPR experiments.[7,41] With PA, an increase of the defect-related lifetime to ~300 ps was observed at 400 K, where the Zn monovacancy anneals out according to EPR.[7,41] This positron lifetime is compatible with divacancies, similar to the lifetime found in as-grown material in Refs. 20 and 22.

Several PA investigations of *n*-type ZnSe layers were reported.[12–14,16] In general, vacancy defects were found, however, no definite assignment to Zn monovacancies could be made due to the lack of positron lifetime measurements. The annihilation parameters were estimated to be $S_V=1.023$ (Refs. 12 and 13) or $S_V=1.029$.[14] It is generally difficult to compare measurements based on the momentum distribution among different groups because the measurement system (most importantly, the energy resolution of the detector) has a significant influence on the results.[42] Nevertheless, our results are in reasonable agreement with that obtained in epitaxial layers (at least for Refs. 12 and 13), corroborating the assignment of defects to V_{Zn} in these studies. This could be finally decided by using bulk samples similar to ours as a reference for the epitaxial layers.

VI. SUMMARY

Positron annihilation spectroscopy was employed to study defects in *n*-type ZnSe. We found vacancies with lifetimes of (280 ± 1) in ZnSe:I or of (275 ± 10) ps in ZnSe:Al and undoped ZnSe at 300 K. These vacancies are identified to be V_{Zn}-donor complexes by combining positron lifetime spectroscopy with measurements of the annihilation momentum distribution. This identification is supported by electron paramagnetic resonance.[23,24] The positron lifetime is in agreement with that found earlier after electron irradiation at low temperature. Our results corroborate the previous assignment of defects in epitaxial *n*-doped ZnSe layers to V_{Zn} by positron annihilation. A quantitative estimation of the vacancy concentration shows that the V_{Zn}-donor complexes can account for the electrical compensation of donors. Our results are in line with the assumption that self-compensation by native vacancies is the dominant compensation mechanism in *n*-type ZnSe.

*Corresponding author. Present address: Lawrence Berkeley National Laboratory, 1 Cyclotron Road, Berkeley, CA 94720. Email address: Jgebauer@lbl.gov

[1] G. F. Neumark, Mater. Sci. Eng., R. **R21**, 46 (1997).
[2] D. B. Laks, C. G. Van de Walle, G. F. Neumark, and S. T. Pantelides, Phys. Rev. Lett. **66**, 648 (1991).
[3] D. B. Laks, C. G. Van de Walle, G. F. Neumark, P. E. Blochl, and S. T. Pantelides, Phys. Rev. B **45**, 10 965 (1992).
[4] S. Pöykkö, M. J. Puska, and R. M. Nieminen, Phys. Rev. B **57**, 12 164 (1998).
[5] S. Pöykkö, M. J. Puska, and R. M. Nieminen, Phys. Rev. B **57**, 12 174 (1998).
[6] D. Y. Jeon, H. P. Gislason, and G. D. Watkins, Phys. Rev. B **48**, 7872 (1993).
[7] G. D. Watkins, in *Radiation Effects in Semiconductors*, edited by N. B. Urli and J. W. Corbett (Gordon and Breach, New York, 1971), p. 301.
[8] K. M. Lee, D. Le Si, and G. D. Watkins, Solid State Commun. **35**, 527 (1980).
[9] W. Schrittenlacher, H. Nelkowski, and H. Pradella, Phys. Status Solidi B **122**, 285 (1984).
[10] D. J. Dunstan, J. E. Nicholls, B. C. Cavenett, and J. J. Davies, J. Phys. C **13**, 6409 (1980).
[11] R. Krause-Rehberg and H. S. Leipner, *Positron Annihilation in Semiconductors* (Springer, Berlin, 1999).
[12] L. Liszkay, C. Corbel, P. Hautojärvi, R. Aulombard, T. Cloitre, J. Griesche, and F. Kiessling, Appl. Phys. Lett. **70**, 2723 (1997).
[13] T. Miyajima, H. Okuyama, K. Akimoto, Y. Mori, L. Wei, and S. Tanigawa, Appl. Phys. Lett. **59**, 1482 (1991).
[14] K. Saarinen, T. Laine, K. Skog, J. Mäkinen, P. Hautojärvi, K. Rakennus, P. Uusimaa, A. Salokatve, and M. Pessa, Phys. Rev. Lett. **77**, 3407 (1996).
[15] J. Oila, K. Saarinen, T. Laine, P. Hautojärvi, P. Uusimaa, M. Pessa, and J. Likonen, Phys. Rev. B **59**, R12 736 (1999).
[16] P. Desgardin, J. Oila, K. Saarinen, P. Hautojärvi, E. Tournie, J. P. Faurie, and C. Corbel, Phys. Rev. B **62**, 15 711 (2000).
[17] M. Alatalo, H. Kauppinen, K. Saarinen, M. J. Puska, J. Mäkinen, P. Hautojärvi, and R. M. Nieminen, Phys. Rev. B **51**, 4176 (1995).
[18] M. Alatalo, B. Barbiellini, M. Hakala, H. Kaupinen, T. Korhonen, M. J. Puska, K. Saarinen, P. Hautojärvi, and R. M. Nieminen, Phys. Rev. B **54**, 2397 (1996).

[19] J. Gebauer, M. Lausmann, T. E. M. Staab, R. Krause-Rehberg, M. Hakala, and M. J. Puska, Phys. Rev. B **60**, 1464 (1999).
[20] G. Tessaro and P. Mascher, J. Cryst. Growth **197**, 581 (1999).
[21] R. Pareja, R. M. d. l. Cruz, and P. Moser, J. Phys.: Condens. Matter **4**, 7153 (1992).
[22] F. Plazaola, K. Saarinen, L. Dobrzynski, H. Reniewicz, F. Firszt, J. Szatkowski, H. Meczynska, S. Legowski, and S. Chabik, J. Appl. Phys. **88**, 1325 (2000).
[23] M. Prokesch, K. Irmscher, J. Gebauer, and R. Krause-Rehberg, J. Cryst. Growth **214-215**, 988 (2000).
[24] K. Irmscher and M. Prokesch, Mater. Sci. Eng., B **80**, 168 (2001).
[25] D. Siche, H. Hartmann, K. Boettcher, and E. Krause, Phys. Status Solidi B **194**, 101 (1996).
[26] R. Krause-Rehberg and H. S. Leipner, Appl. Phys. A: Mater. Sci. Process. **64**, 457 (1997).
[27] J. Gebauer, R. Krause-Rehberg, S. Eichler, and F. Börner, Appl. Surf. Sci. **149**, 110 (1999).
[28] J. Gebauer, R. Krause-Rehberg, and T. E. M. Staab, Phys. Status Solidi B **220**, R1 (2000).
[29] *Properties of Wide Bandgap II-VI Semiconductors*, edited by R. Bhargava (INSPEC, London, 1997).
[30] K. Saarinen, P. Hautojärvi, A. Vehanen, R. Krause, and G. Dlubek, Phys. Rev. B **39**, 5287 (1989).
[31] S. Dannefaer and A. Pu, Nucl. Instrum. Methods Phys. Res. A **462**, 596 (2001).
[32] M. J. Puska, C. Corbel, and R. M. Nieminen, Phys. Rev. B **41**, 9980 (1990).
[33] H. Kauppinen, L. Baroux, K. Saarinen, C. Corbel, and P. Hautojärvi, J. Phys.: Condens. Matter **9**, 5495 (1997).
[34] U. Myler, R. D. Goldberg, A. P. Knights, D. W. Lawther, and P. J. Simpson, Appl. Phys. Lett. **69**, 3333 (1996).
[35] T. Abgarjan, Ph.D. thesis, Martin-Luther-Universität, 1994; R. Krause-Rehberg, H. S. Leipner, T. Abgarjan, and A. Polity, Appl. Phys. A: Mater. Sci. Process. **66**, 599 (1998).
[36] S. B. Zhang and J. E. Northrup, Phys. Rev. Lett. **67**, 2339 (1991); T. Y. Tan, H. M. You, and U. M. Gösele, Appl. Phys. A: Mater. Sci. Process. **56**, 249 (1993).
[37] D. T. J. Hurle, J. Appl. Phys. **85**, 6957 (1999).
[38] F. Plazaola, A. P. Seitsonen, and M. J. Puska, J. Phys.: Condens. Matter **6**, 8809 (1994).
[39] B. Barbiellini, M. J. Puska, T. Korhonen, A. Harju, T. Torsti, and R. M. Nieminen, Phys. Rev. B **53**, 16 201 (1996).
[40] M. J. Puska, A. P. Seitsonen, and R. M. Nieminen, Phys. Rev. B **52**, 10 947 (1995).
[41] K. M. Lee, K. P. O'Donnell, and G. D. Watkins, Solid State Commun. **41**, 881 (1982).
[42] S. Eichler and R. Krause-Rehberg, Appl. Surf. Sci. **149**, 227 (1999).